



1 **Snow data intercomparison on remote and glacierized high elevation**
2 **areas (Forni Glacier, Italy)**
3

4 Senese Antonella¹, Maugeri Maurizio¹, Meraldi Eraldo², Verza Giampietro³, Azzoni Roberto Sergio¹,
5 Compostella Chiara⁴, Diolaiuti Guglielmina¹

6 ¹ Department of Environmental Science and Policy, Università degli Studi di Milano, Milan, Italy.

7 ² ARPA Lombardia, Centro Nivometeorologico di Bormio, Bormio, Italy.

8 ³ Ev-K2-CNR - Pakistan, Italian K2 Museum Skardu Gilgit Baltistan, Islamabad, Pakistan.

9 ⁴ Department of Earth Sciences, Università degli Studi di Milano, Milan, Italy.
10

11 *Correspondence to:* Antonella Senese (antonella.senese@unimi.it)

12

13 **Abstract.**

14 We present and compare 11 years of snow data (snowfall, snow depth and snow water equivalent (*SWE*)) measured by an
15 Automatic Weather Station and by some field campaigns on the Forni Glacier. The data have been acquired by means of i) a
16 Campbell SR50 sonic ranger from October 2005 (snow depth data), ii) manual snow pits from January 2006 (snow depth and
17 *SWE* data), iii) a Sommer USH8 sonic ranger from May 2014 (snow depth data), iv) a Park Mechanical SS-6048 snow pillow
18 from May 2014 (*SWE* data), v) a manual snow weighting tube (Enel-Valtecne ©) from May 2014 (snow depth and *SWE* data).
19 The aim of the analyses is to assess the mean value of fresh snow density and the most appropriate method to evaluate *SWE*
20 for this measuring site.

21 The results indicate that the daily SR50 sonic ranger measures allow a rather good estimation of the *SWE*, and the provided
22 snow pit data are available for defining the site mean value of fresh snow density. For the Forni Glacier measuring site, this
23 value turned out to be 140 kg m⁻³. The *SWE* derived from sonic ranger data is rather sensitive to this value: a change in fresh
24 snow density of 20 kg m⁻³ causes a mean variation in *SWE* of ±0.093 m w.e. for each hydrological year, ranging from ±0.050
25 m w.e. to ±0.115 m w.e..
26

27 **Keywords:** Snow depth; Snow water equivalent (*SWE*); SPICE (Solid Precipitation Intercomparison Experiment) project;
28 Forni Glacier.
29

30

31 **1. Introduction and scientific background**

32 The study of spatial and temporal variability of the water resource deriving from snow melt (i.e. Snow Water Equivalent,
33 *SWE*) is very important for the estimation of the hydrological balance at catchment scale. In particular, many areas depend on
34 this water reservoir for providing freshwater for civil use, irrigation and hydropower thus requiring an accurate and updated



35 evaluation of *SWE* magnitude and variability. In addition, a correct *SWE* assessment also supports early strategies to manage
36 and prevent hydro-meteorological risks (e.g. flood forecasting, avalanche forecasting).

37 In high mountain areas, however, only snowfall measures are often available: a correct evaluation of fresh snow density
38 ($\rho_{fresh\ snow}$) is therefore needed to assess the *SWE*. Since fresh snow density is site specific and depending on atmospheric
39 conditions, the main aim of this study is to investigate magnitude and rates of variations in $\rho_{fresh\ snow}$ and to understand how an
40 incorrect assessment of this variable may affect the estimation of the *SWE*. This was possible by means of manual and
41 automatic systematic measurements carried out at the surface of the Forni Glacier (Stelvio Park, Italian Alps, Fig. 1a and b).
42 The Forni Glacier is a Site of Community Importance (SCI, code IT2040014) located inside a wide natural protected area (i.e.
43 the Stelvio Park). It is a wide valley glacier (ca. 11.34 km² of area, D'Agata et al., 2014), covering an elevation range from
44 2600 to 3670 m a.s.l.. From 2005, an Automatic Weather Station (AWS1 Forni) has been acquiring snow data at the glacier
45 surface in addition to measurements of snow depth and *SWE* by means of snow pits carried out by expert personnel (Citterio
46 et al., 2007; Senese et al., 2012a; 2012b; 2014). The acquired snow data refer to snowfall or fresh-snow (i.e. depth of freshly
47 fallen snow deposited over a specified period, generally 24 hours, see WMO, 2008) and to snow depth (i.e. the total depth of
48 snow on the ground at the time of observation, see WMO, 2008). The long sequence of meteorological and glaciological data
49 permitted the insertion of the AWS1 Forni into SPICE (Solid Precipitation Intercomparison Experiment) project managed
50 and promoted by the WMO (World Meteorological Organization) and CryoNet project (core network of Global Cryosphere
51 Watch promoted by the WMO).

52 Fresh snow-density assessment is important also for snowfall forecasting from orographic precipitation models (Judson and
53 Doesken, 2000; Roebber et al., 2003), estimation of avalanche hazard (Perla, 1970; LaChapelle, 1980; Ferguson et al., 1990;
54 McClung and Schaerer, 1993), snowdrift forecasting, as an input parameter in the snow accumulation algorithm (Super and
55 Holroyd, 1997), and general snow science research.

56 Following Roebber et al. (2003), fresh snow density is often assumed to conform to the 10-to-1 rule: the snow ratio, defined
57 by the density of water (1000 kg m⁻³) to the density of fresh snow (assumed to be 100 kg m⁻³), is 10:1. As noted by Judson
58 and Doesken (2000), the 10-to-1 rule appears to originate from the results of a nineteenth-century Canadian study. More
59 comprehensive measurements of fresh snow density (e.g., Currie, 1947; LaChapelle, 1962; Power et al., 1964; Super and
60 Holroyd, 1997; Judson and Doesken, 2000) have established that this rule is an inadequate characterization of the true range
61 of fresh snow densities. Indeed, they can vary from 10 kg m⁻³ to approximately 350 kg m⁻³ (Roebber et al., 2003). Bocchiola
62 and Rosso (2007) report a similar range for the Central Italian Alps with values ranging from 30 kg m⁻³ to 480 kg m⁻³, with
63 an average sample value of 123 kg m⁻³. Usually, the density of fresh snow is lower bounded to about 50 kg m⁻³ (Gray, 1979;
64 Anderson and Crawford, 1990). Judson and Doesken (2000) found densities of fresh snow observed from six sheltered
65 avalanche sites in the Central Rocky Mountains to range from 10 to 257 kg m⁻³ and average densities at each site based on
66 four years of daily observations to range from 72 to 103 kg m⁻³. Roebber et al. (2003) found that the 10-to-1 rule may be
67 modified slightly to 12 to 1 or 20 to 1, depending on the mean or median climatological value of fresh snow density at a
68 particular station (e.g. Currie 1947; Super and Holroyd, 1997). Following Pahaut (1975), the fresh snow density ranges from
69 20 to 200 kg m⁻³ and increases with wind speed and air temperature. Wetzel and Martin (2001) analyzed all empirical
70 techniques evolved in the absence of explicit snow-density forecasts. As argued in Schultz et al. (2002), however, these
71 techniques might be not fully adequate and the accuracy should be verified in details for a large variety of events.



72 Fresh snow density is regulated by i) in-cloud processes that affect the shape and size of growing ice crystals, ii) sub-cloud
73 thermodynamic stratification through which an ice crystal falls (i.e. the low-level air temperature and relative humidity
74 regulate the processes of sublimation or melting of a snowflake), and iii) ground-level compaction due to prevailing weather
75 conditions and snowpack metamorphism. Understanding how these processes affect fresh snow density is difficult because
76 direct observations of cloud microphysical processes, thermodynamic profiles, and surface measurements are often
77 unavailable.

78 Cloud microphysical research indicates that many factors contribute to the final structure of an ice crystal. The shape of the
79 ice crystal is determined by the environment in which the ice crystal grows: pure dendrites have the lowest density (Power et
80 al., 1964), although the variation in the density of dendritic aggregates is large (from approximately 5 to 100 kg m⁻³, Magono
81 and Nakamura, 1965; Passarelli and Srivastava, 1979). Numerous observational studies over decades clearly demonstrate that
82 the density varies inversely with size (Magono and Nakamura, 1965; Holroyd, 1971; Muramoto et al., 1995; Fabry and
83 Szyrmer, 1999; Heymsfield et al., 2004; Brandes et al., 2007). The crystal size is related to the ratio between ice and air
84 (Roebber et al., 2003): large dendritic crystals will occupy much empty air space, whereas smaller crystals will pack together
85 into a denser assemblage. In addition, as an ice crystal falls, it passes through varying thermodynamic and moisture conditions.
86 Then, the ultimate shape and size of crystals depend on factors that affect the growth rate and are a combination of various
87 growth modes (e.g. Pruppacher and Klett, 1997).

88 To contribute to the understanding of all the above topics, in this paper we discuss and compare all the available snow data
89 measured at the Forni Glacier surface in the last decade to: i) suggest the most suitable measurement method to evaluate *SWE*
90 at a glacier surface (i.e. snow pillow or sonic ranger or snow pits); ii) define the reliability of the obtained *SWE* values and
91 their accuracies; iii) check the validity of the $\rho_{fresh\ snow}$ value previously found (i.e. 140 kg m⁻³, see Senese et al., 2014) to
92 support *SWE* computation; and iv) evaluate effects and impacts of uncertainties in the $\rho_{fresh\ snow}$ value in the derived *SWE*
93 amount.

94

95

96 2. Data and Methods

97 Snow data at the Forni Glacier have been acquired by means of i) a Campbell SR50 sonic ranger from October 2005 (snow
98 depth data), ii) manual snow pits from January 2006 (snow depth and *SWE* data), iii) a Sommer USH8 sonic ranger from May
99 2014 (snow depth data), iv) a Park Mechanical SS-6048 snow pillow from May 2014 (*SWE* data), v) a manual snow weighting
100 tube (Enel-Valtece ©) from May 2014 (snow depth and *SWE* data). These sensors are installed at two automatic weather
101 stations (AWSs): AWS1 Forni and AWS Forni SPICE. The first station (named AWS1 Forni, Fig. 1b) was installed on 26th
102 September 2005 at the lower sector of the Forni Glacier eastern tongue (Citterio et al., 2007; Senese et al., 2012a, 2012b;
103 2014; 2016). The WGS84 coordinates of AWS1 Forni are: 46° 23' 56.0" N, 10° 35' 25.2" E, 2631 m a.s.l. (Fig. 1a, yellow
104 triangle). The second station (named AWS Forni SPICE, Fig. 1b) was installed on 6th May 2014 close to the AWS1 Forni (at
105 a distance of 17 m).

106 The AWS1 Forni is equipped with sensors for measuring air temperature and humidity (naturally ventilated sensor), wind
107 speed and direction, air pressure, and the four components of the radiation budget (longwave and shortwave, both incoming
108 and outgoing fluxes), liquid precipitation, and snow depth by means of the Campbell SR50 sonic ranger (Table 1, see also
109 Senese et al., 2012a).



110 The AWS Forni SPICE is equipped with sensors for measuring also the snow water equivalent by means of the snow pillow
111 and the air pressure (Table 1). This latter permits to calibrate the output values recorded by the snow pillow. The pressure
112 snow pillow gauge is a device similar to a large air or water mattress filled with antifreeze. As snow is deposited on this gauge,
113 the pressure increase is related to the accumulating mass and thus to *SWE*. On the mast, an automated camera was installed
114 to photograph four graduated stakes located at the corners of the snow pillow (Fig. 1b). When the snow pillow was installed,
115 a second sonic ranger (Sommer USH8) was installed on the AWS1 Forni.

116 The main constrictions in installing and managing AWS1 Forni and AWS Forni SPICE were due to the fact that the site is
117 located on the surface of an Alpine glacier, not always accessible, especially during wintertime when skis and skins are needed
118 on the steep and narrow path, and avalanches can occur. Moreover, the glacier is a dynamic body (moving up to 20-30 m y⁻¹,
119 Urbini et al., 2017) and its surface also features a well-developed roughness due to ice melting, flowing meltwater, differential
120 ablation and opening crevasses (Diolaiuti and Smiraglia, 2010; Smiraglia and Diolaiuti, 2011). In addition, the power to be
121 supplied to instruments and sensors is only represented by solar panels and lead-gel batteries. Then, a deep and accurate
122 analysis of instruments and devices (i.e. energy supply required, performance and efficiency working at low temperatures,
123 noise in measuring due to ice flow, etc.) before their installation on the supraglacial AWS is necessary to avoid interruptions
124 in data acquisition and storage.

125 As regards the AWS1 Forni, two data loggers are installed: a LSI-Lastem Babuc ABC (in 2005) and a Campbell Scientific
126 CR200 (in 2014). This latter allows the correct working of the Young wind sensor and the Sommer sonic ranger. All the other
127 sensors are connected to the LSI-Lastem Babuc ABC. A Campbell Scientific CR1000 was installed at the AWS Forni SPICE
128 (in 2014).

129 The whole systems of both AWS1 Forni and AWS Forni SPICE are supported by four-leg stainless steel masts (5 m and 6 m
130 high, respectively) standing on the ice surface. In this way, the AWSs stand freely on the ice, and adjust to the melting surface
131 during summer.

132 Due to the formation of ring faults that could compromise the stability of the stations (Azzoni et al., submitted), in November
133 2015 both AWSs were moved to the Forni glacier central tongue (46°23'42.40"N and 10°35'24.20"E at an elevation of 2675
134 m a.s.l., the red star in Fig. 1a).

135 In addition, since winter 2005/2006, personnel from the Centro Nivo-Meteorologico (namely CNM Bormio-ARPA
136 Lombardia) of the Lombardy Regional Agency for the Environment have been carrying out periodic snow pits (performed
137 according to the AINEVA protocol, see also Senese et al., 2014) in order to estimate snow depth and *SWE*. In particular, the
138 thickness (h_i) and the density (ρ_i) of each snow layer (i) are measured for estimating the snow water equivalent of each layer
139 and then the total $SWE_{snow-pit}$ of the whole snow cover (n layers):

$$140 \quad SWE_{snow-pit} = \sum_{i=1}^n h_i \cdot \frac{\rho_i}{\rho_{water}} \quad (1)$$

141 where ρ_{water} is density of water. As stated in a previous study (Senese et al., 2014), the date when the snow pit is dug is very
142 important for not underestimating the actual accumulation. For this reason, we considered only the snow pits carried out
143 before the beginning of snow ablation. In fact, whenever ablation occurs, successive *SWE* values derived from snow pits show
144 a decreasing trend (i.e. they are affected by mass losses). In these cases, we considered the highest *SWE* value, before the
145 occurrence of snow ablation.

146 *SWE* values are also estimated from snow depth data acquired by sonic rangers. In particular, daily positive differences in
147 depth (Δh) are considered:



$$148 \quad SWE_{sonic-ranger} = \sum_{t=1}^m (\Delta h_t) \cdot \frac{\rho_{fresh\ snow}}{\rho_{water}} \quad (2)$$

149 where m is the total number of snow days and $\rho_{fresh\ snow}$ is the fresh snow density.

150 The optimal value of $\rho_{fresh\ snow}$ is then found by comparing SWE from sonic rangers (where fresh snow density is the unique
151 unknown parameter but the record of data is generally continuous and uninterrupted thus recording all the snowfall events)
152 against SWE from snow pits (where snow density is sampled at each layer but these measurements are performed in a unique
153 date).

154 In previous analyses performed using Forni Glacier data, we have obtained the best match against the two data series by
155 applying a $\rho_{fresh\ snow}$ value of 140 kg m^{-3} (see Citterio et al., 2007; Senese et al., 2012a; 2014).

156

157

158 3. Results

159 Figure 2 represents the 11-year dataset of snow depth measured by the sonic ranger SR50 from 2005 to 2016. The last data
160 (after October 2015) were recorded in a different site than the previous one because of the AWSs displacement of November
161 2015.

162 A large interannual variability is seen with the maximum peak of 2.80 m (on 2nd May 2008). In general, the snow depth
163 exceeds 2 m, except in 2006-2007 period, which is characterized by the lowest maximum value (1.34 m on 26th March 2007).

164 The snow accumulation period generally starts between the end of September and the beginning of October. Whereas, the
165 snow appears to be completely melted between the half of June and the beginning of July (Fig. 2).

166 During the last two years, data from the sonic ranger Sommer USH8 were also available even if with some gaps (26% of the
167 total period). Comparing the datasets from Campbell and Sommer sensors, a very good agreement is found (Fig. 3). This
168 means that in spite of some problems in recording Sommer sonic ranger data, both sensors worked correctly and all the
169 snowfalls were properly recognized.

170 Because of the not complete dataset from the sonic ranger Sommer USH8, the following analyses are however performed
171 considering only the Campbell SR50 sensor.

172 Figure 4 reports the comparison between the sonic ranger-derived SWE values (i.e. applying Eq. (2) and using a fresh snow
173 density of 140 kg m^{-3}) and the ones obtained by snow pits from 2005 to 2016. As found in previous studies (Senese et al.,
174 2012a, 2014), there is a very good agreement between the two series of data (i.e. snow-pit-measured and sonic-ranger-derived
175 SWE). Whenever sonic ranger data are not available for a long period, the derived total SWE value results to be incorrect. In
176 particular, it is clear that the period of the year without data is very important for not underestimating the actual accumulation.

177 During the snow accumulation period 2010-2011, the data gap from 15 December 2010 to 12 February 2011 (totally 60 days)
178 produces an underestimation of 0.163 m w.e. (on 25th April 2011 derived $SWE = 0.607$ and measured $SWE = 0.770$, Fig. 4).

179 During the hydrological years 2011-2012 and 2012-2013, there were some problems with sonic ranger data acquisition thus
180 making impossible to elaborate these data from 31st January 2012 to 25th April 2013. In these cases, there are noticeable
181 differences between the two series of data: on 1st May 2012 measured $SWE = 0.615$ m w.e. and derived $SWE = 0.238$ m w.e.,
182 and on 25th April 2013 measured $SWE = 0.778$ m w.e. and derived $SWE = 0.307$ m w.e., Fig. 4). Therefore, whenever the
183 recorded data are not available from February, the derived SWE could not be considered adequate and generally equal to the
184 half of the total value.



185 Figure 5 reports the comparison between the sonic ranger-derived SWE values and the ones obtained by the snow pillow
186 (2014-2016 period). From this graph, it is evident that the snow pillow has some measuring problems at the beginning of the
187 snow season when snow cover is low. Except this first period without snow, the curve of SWE measured by the snow pillow
188 follows the sonic ranger-derived SWE curve (Fig. 5), thus suggesting a correct working of the sensor. In order to better assess
189 the reliability of our derived SWE values, a scatter plot of measured versus derived SWE data is shown (Fig. 6). The chosen
190 period is the snow accumulation time frame during 2014/2015 and 2015/2016: from November 2014 to March 2015 and from
191 February 2016 to May 2016 (i.e. excluding the initial period in which the snow pillow seems to have relevant measuring
192 problems, to the moment before the beginning of snow ablation, see Fig 3). There is a general underestimation of derided
193 SWE from SR50 compared to the ones measured by both snow pillow and snow pit considering data of 2014/2015, however
194 the agreement raises with 2015/2016 dataset (Fig. 6). The root mean square error is 0.051 m w.e. if compared with snow
195 pillow dataset, and the difference with the snow pit is 0.067 m w.e. Nevertheless, carrying out numerous measurements
196 through the snow weighting tube (Enel-Valtecnica ©) around the AWSs on 20th February 2015, a large spatial variability of
197 snow depth was found even if the snow surface seemed to be homogenous. This was mainly due to the roughness of the
198 glacier ice surface. Indeed, on 20th February 2015 the snow pillow recorded a SWE value of 0.493 m w.e., while from the
199 snow pit the SWE resulted equal to 0.555 m w.e., and from the snow weighing tube the SWE ranged from 0.410 to 0.552 m
200 w.e., even if all measurements were performed very close to each other. In addition, this difference can be also due to
201 oversampling by the snow tube (Work et al., 1965).

202
203

204 4. Discussions

205 Once verified our procedure, we performed further tests in order to define the SWE sensitivity with changing the fresh snow
206 density (Fig. 7). An increase/decrease of 20 kg m⁻³ causes a mean variation in SWE of ±0.093 m w.e. for each hydrological
207 year, ranging from ±0.050 m w.e. to ±0.115 m w.e. From this analysis, using a density value of 140 kg m⁻³ is confirmed to be
208 the best one compared with SWE values measured by snow pits (Table 2).

209 Beside to a general good agreement between the measures performed with the different sensors, there are also some problems.
210 Focusing only on the beginning of the snow accumulation period, it appears that all sensors (i.e. sonic ranger and snow pillow)
211 are not able to correctly detect the first snowfall events. As regards sonic ranger, the surface roughness of the glacier ice does
212 not allow to distinguish a few centimeters of fresh snow, as it causes differences in surface elevation up to tens of centimeters
213 and affects the angular distribution of reflected ultrasound. At 3 m of height, the diameter of measuring field is 1.17 m and
214 0.63 m for SR50 and USH8, respectively. For these reasons, the sonic ranger generally records not constant distances between
215 ice surface and sensor. This issue does not occur with thick snow cover as the snow roughness is very small compared to the
216 ice one. In order to assess the beginning of the snow accumulation period, albedo represents a useful tool as fresh snow and
217 ice are characterized by very different values (e.g. Azzoni et al., 2016). In fact, whenever a snowfall event occurs, albedo
218 immediately raises from about 0.2 to 0.9 (typical values of ice and fresh snow, respectively, Senese et al., 2012a). This is
219 confirmed also by the pictures taken hourly by the AWSs automated camera. During the hydrological year 2014/2015, the
220 first snowfall was detected on 22nd October 2014 by analyzing albedo data and it is verified by pictures taken by the automated
221 camera. Before this date, the sonic ranger does not recorded a null snow depth mainly due to the ice roughness and then we
222 had to correct the dataset accordingly.



223 Regarding snow pillow, some of the under-measurement or over-measurement errors can be attributed to differences in the
224 amount of snow settlement over the snow pillow compared with the surrounding ground, or to bridging over the snow pillow
225 with cold conditions during development of the snow cover (Beaumont, 1965). The dominant source of *SWE* snow pillow
226 errors is generally due to measuring problems of this device, which is sensitive to the thermal conditions of the sensor, the
227 ground and the snow (Johnson et al., 2015). In fact, according to Johnson and Schaefer (2002) and Johnson (2004) snow
228 pillow under-measurement and over-measurement errors can be related to the amount of heat conduction from the ground
229 into the overlying snow cover, the temperature at the ground/snow interface and the insulating effect of the overlying snow.
230 Analyzing 2014/2015 and 2015/2016 data, the snow pillow seems to be working correctly only with snow cover thicker than
231 50 cm (Fig. 5).

232 In general, the precipitation can be acquired mechanically, optically, in capacitive way and by means of radar. Some examples
233 of available sensors are: heated tipping bucket rain gauge (as precipitation is collected and melted in the gauge's funnel, water
234 is directed to a tipping bucket mechanism adjusted to tip and dump when a volume threshold of water is collected), heated
235 weighing gauge (the weight of water collected is measured as a function of time and converted to rainfall depth), disdrometer
236 (measuring the drop size distribution and velocity of falling hydrometeors), snow water equivalent sensor based on the
237 attenuation of the electromagnetic energy from the ground (by passively detecting the change in naturally occurring
238 electromagnetic energy from the ground after it passes through snow cover). In particular, for the Solid Precipitation
239 Intercomparison Experiment (1989-1993), the International Organizing Committee designated the following method as the
240 reference for the Intercomparison and named it as the Double Fence Intercomparison Reference (DFIR): "The octagonal
241 vertical double-fence inscribed into circles 12 m and 4 m in diameter, with the outer fence 3.5 m high and the inner fence 3.0
242 m high surrounding a Tretyakov precipitation gauge mounted at a height of 3.0 m. In the outer fence there is a gap of 2.0 m
243 and in the inner fence of 1.5 m between the ground and the bottom of the fences." (WMO/TD-872/1998, section 2.2.2). In
244 remote areas like a glacier, it is however very difficult to install and maintain such sensors. One of the constrictions concerns
245 the power to be supplied to instruments that is represented only by solar panels and lead-gel batteries. In fact, at the Forni site
246 we had to choose only unheated low-power sensors. The snow pillow turned out to be logistically unsuitable, as it required
247 frequent maintenance. Especially with bare ice or few centimeters of snow cover, the differential ablation causes instability
248 of the snow pillow mainly due to its size. In addition, it is not able to detect *SWE* lower than about 0.2 m w.e. (corresponding
249 to a snow depth of about 50 cm). Therefore, this sensor is resulted to be a tool not appropriate for a glacier surface or a remote
250 area in general. The snow pit can represent a useful approach but it requires expert personnel for carrying out the measurement.
251 Moreover, as discussed in Senese et al. (2014), it is very important to select a correct date for performing snow pits in order
252 to assess the whole glacier accumulation amount. Generally, 1st April is the date largely considered as the most indicative of
253 the cumulative *SWE* in high mountain environments of the midlatitudes, but this date is not always the best one. In fact, Senese
254 et al. (2014) found that using a fixed date for measuring the total *SWE* is not the most suitable solution. In particular, they
255 suggest that a correct temperature threshold can help in detecting the most appropriate time window of analysis indicating the
256 starting time of snow melting processes and then the end of the accumulation period. The automated camera provided hourly
257 photos but for assessing a correct snow depth at least two graduated rods have to be installed closed to the automated camera.
258 Over a glacier surface, glacier dynamics and snow flux can compromise the stability of the rods: in fact, after a short while
259 we found them broken at the AWS Forni SPICE. Finally, with data acquired by the SR50 sonic ranger a correct curve of *SWE*
260 was derived. The unique issue is represented by the definition of the beginning of the accumulation period, but this can be



261 overcome using albedo data. Unlike SR50 sensor, USH8 sonic ranger showed more problems and then less available data that
262 did not make possible to calculate *SWE* values. Therefore, SR50 sonic ranger turned out to be the most suitable device in
263 order to define both snow depth and daily cumulative *SWE* (as the fresh snow density is defined).

264

265

266 5. Conclusions

267 In occasion of the SPICE (Solid Precipitation Intercomparison Experiment) project, at the Forni Glacier (Italian Alps) snow
268 measurements have been carried out by means of several automatic and manual approaches from 2014. This has allowed an
269 accurate comparison and evaluation of pros and cons in using snow pillow or sonic ranger or manual snow pit and snow
270 weighting tube. The results achieved during the SPICE experiment support our procedure for deriving *SWE* values and the
271 applied fresh snow density of 140 kg m^{-3} (Senese et al., 2014), and suggest that, once $\rho_{\text{fresh snow}}$ is known, the SR50 sonic
272 ranger can be considered the most suitable device on a glacier to record snowfall events and to measure snow depth values in
273 order to derive the point *SWE*. Moreover, we evaluated effects and impacts of changing $\rho_{\text{fresh snow}}$ value in the derived *SWE*
274 amount and we found that a slight change in density of 20 kg m^{-3} causes a mean variation in *SWE* of $\pm 0.093 \text{ m w.e.}$ for each
275 hydrological year, ranging from $\pm 0.050 \text{ m w.e.}$ to $\pm 0.115 \text{ m w.e.}$

276

277

278 Acknowledgements

279 The AWS1 Forni was developed under the umbrella of the SHARE (Stations at High Altitude for Research on the
280 Environment) program, managed by the Ev-K2-CNR Association from 2002 to 2014; it was part of the former CEOP network
281 (Coordinated Energy and Water Cycle Observation Project) promoted by the WCRP (World Climate Research Programme)
282 within the framework of the online GEWEX project (Global Energy and Water Cycle Experiment); it was inserted in the
283 SPICE (Solid Precipitation Intercomparison Experiment) project managed and promoted by the WMO (World Meteorological
284 Organization), and in the CryoNet project (core network of Global Cryosphere Watch promoted by the WMO), and it was
285 applied in the ESSEM COST Action ES1404 (a European network for a harmonised monitoring of snow for the benefit of
286 climate change scenarios, hydrology and numerical weather prediction).

287 This research was achieved under the umbrella of a research project funded by Sanpellegrino Levissima Spa and young
288 researchers involved in the study were supported by DARAS (Department of regional affairs, autonomies and sport) of the
289 Presidency of the Council of Ministers of the Italian government through the GlacioVAR project (PI G. Diolaiuti). Moreover,
290 the Stelvio Park - ERSAF kindly supported data analyses and has been hosting the AWS1 Forni and the AWS SPICE at the
291 surface of the Forni Glacier thus permitting the beginning of the glacier micro-meteorology in Italy.

292

293

294 References

295 Anderson, E.A. and Crawford, N.H.: The synthesis of continuous snowmelt hydrographs on digital computer. Tech. Rep. n.
296 36, Department Of Civil Engineering of the Stanford university, as reported in: Bras, 1990; 1964.



- 297 Azzoni, R.S., Senese, A., Zerboni, A., Maugeri, M., Smiraglia, C., and Diolaiuti, G.: Estimating ice albedo from fine debris
298 cover quantified by a semi-automatic method: the case study of Forni Glacier, Italian Alps. *The Cryosphere*, 10, 665–679.
299 2016doi:10.5194/tc-10-665-2016. Available online at <http://www.the-cryosphere.net/10/665/2016/tc-10-665-2016.pdf>
300 Azzoni, R.S., Fugazza, D., Zennaro, M., Zucali, M., D'Agata, C., Maragno, M., Smiraglia, C., and Diolaiuti, G.A.: Recent
301 structural evolution of Forni Glacier tongue (Ortles-Cevedale Group, Central Italian Alps). Submitted to *Journal of Maps*.
302
303 Beaumont, R.T.: Mt. Hood pressure pillow snow gauge, *J. Appl. Meteorol.*, 4, 626–631, 1965.
304
305 Bocchiola, D. and Rosso, R.: The distribution of daily snow water equivalent in the central Italian Alps. *Advances in Water*
306 *Resources* 30 (2007) 135–147, 2007.
307
308 Brandes, E.A., Ikeda, K., Zhang, G., Schonhuber, M., and Rasmussen, R.M.: A statistical and physical description of
309 hydrometeor distributions in Colorado snowstorms using a video disdrometer. *J. Appl. Meteor. Climatol.*, 46, 634–650,
310 2007.
311
312 Citterio, M., Diolaiuti, G., Smiraglia, C., Verza, G., and Meraldi, E.: Initial results from the automatic weather station (AWS)
313 on the ablation tongue of Forni Glacier (Upper Valtellina, Italy), *Geogr. Fis. Din. Quat.*, 30, 141–151, 2007.
314
315 Currie, B. W., 1947: Water content of snow in cold climates. *Bull. Amer. Meteor. Soc.*, 28, 150–151.
316
317 D'Agata, C., Bocchiola, D., Maragno, D., Smiraglia, C., and Diolaiuti, G.A.: Glacier shrinkage driven by climate change in
318 The Ortles-Cevedale group (Stelvio National Park, Lombardy, Italian Alps) during half a century (1954–2007).
319 *Theoretical Applied Climatology*, April 2014, Volume 116, Issue 1–2, pp 169–190, 2014.
320 <http://link.springer.com/article/10.1007/s00704-013-0938-5>
321
322 Diolaiuti, G. and Smiraglia, C.: Changing glaciers in a changing climate: how vanishing geomorphosites have been
323 driving deep changes in mountain landscapes and environments, *Geomorphologie*, 2, 131–152, 2010.
324
325 Fabry, F. and Szyrmer, W.: Modeling of the melting layer. Part II: Electromagnetic. *J. Atmos. Sci.*, 56, 3593–3600, 1999.
326
327 Ferguson, S. A., Moore, M.B., Marriott, R.T., and Speers-Hayes, P.: Avalanche weather forecasting at the northwest
328 avalanche center, Seattle, WA. *J. Glaciol.*, 36, 57–66, 1990.
329
330 Gray, D.M.: Snow accumulation and distribution. In: Colbeck SC, Ray M, eds., *Proceedings: proceedings, modeling of snow*
331 *cover runoff*, Hanover, NH, 3–33, 1979.
332
333 Heymsfield, A.J., Bansemmer, A., Schmitt, C., Twohy, C., and Poellot, M.R.: Effective ice particle densities derived from
aircraft data. *J. Atmos. Sci.*, 61, 982–1003, 2004.
Holroyd, E.W., III: The meso- and microscale structure of Great Lakes snowstorm bands: A synthesis of ground
measurements, radar data, and satellite observations. Ph.D. dissertation, University at Albany, State University of New
York, 148 pp, 1971.
Johnson, J.B. and Schaefer, G.: The influence of thermal, hydrologic, and snow deformation mechanisms on snow water
equivalent pressure sensor accuracy. *Hydrological Processes* 16: 3529–3542, 2002.
Johnson, J.B.: A theory of pressure sensor performance in snow. *Hydrological Processes* 18, 53–64, 2004.
Johnson, J.B., Gelvin, A.B., Duvoy, P., Schaefer, G.L., Poole, G., and Horton, G.D.: Performance characteristics of a new
electronic snow water equivalent sensor in different climates. *Hydrological Processes*, 29(6), 1418–1433, 2015.
Judson, A. and Doesken, N.: Density of freshly fallen snow in the central Rocky Mountains. *Bull. Amer. Meteor. Soc.*, 81,
1577–1587, 2000.



- 334 LaChapelle, E.R.: The density distribution of new snow. Project F, Progress Rep. 2, USDA Forest Service, Wasatch National
335 Forest, Alta Avalanche Study Center, Salt Lake City, UT, 13 pp, 1962.
- 336 LaChapelle, E.R.: The fundamental process in conventional avalanche forecasting. *J. Glaciol.*, 26, 75–84, 1980.
- 337 Magono, C. and Nakamura, T.: Aerodynamic studies of falling snow flakes. *J. Meteor. Soc. Japan*, 43, 139–147, 1965.
- 338 McClung, D.M. and Schaerer, P.A.: The avalanche handbook. Seattle, WA, The Mountaineers, 1993.
- 339 Muramoto, K.I., Matsuura, K., and Shiina, T.: Measuring the density of snow particles and snowfall rate. *Electron. Commun.*
340 *Japan*, 78, 71–79, 1995.
- 341 Nolin, A.W., Fetterer, F.M., and Scambos, T.A.: Surface roughness characterizations of sea ice and ice sheets: Case studies
342 with MISR data. *IEEE transactions on Geoscience and Remote Sensing*, 40(7), 1605–1615, 2002.
- 343 Pahaut, E.: Les cristaux de neige et leurs metamorphoses. *Monographies de la Meteorologie Nationale*, 1975.
- 344 Passarelli, R.E.Jr. and Srivastava, R.C.: A new aspect of snowflake aggregation theory. *J. Atmos. Sci.*, 36, 484–493, 1979.
- 345 Perla, R.: On contributory factors in avalanche hazard evaluation. *Can. Geotech. J.*, 7, 414–419, 1970.
- 346 Power, B.A., Summers, P.W., and d’Avignon, J.: Snow crystal forms and riming effects as related to snowfall density and
347 general storm conditions. *J. Atmos. Sci.*, 21, 300–305, 1964.
- 348 Pruppacher, H.R. and Klett, J.D.: *Microphysics of Clouds and Precipitation*. 2d ed. Kluwer Academic, 954 pp, 1997.
- 349 Roebber, P.J., Bruening, S.L., Schultz, D.M., and Cortinas Jr, J.V.: Improving snowfall forecasting by diagnosing snow
350 density. *Weather and Forecasting*, 18(2), 264–287, 2003.
- 351 Schultz, D.M., Cortinas Jr, J.V., and Doswell III, C.A.: Comments on “An operational ingredients-based methodology for
352 forecasting midlatitude winter season precipitation.” *Wea. Forecasting*, 17, 160–167, 2002.
- 353 Senese, A., Diolaiuti, G., Mihalcea, C., and Smiraglia, C.: Energy and mass balance of Forni Glacier (Stelvio National Park,
354 Italian Alps) from a 4-year meteorological data record. *Arct. Antarct. Alp. Res.*, 44, 122–134, 2012a.
- 355 Senese, A., Diolaiuti, G., Verza, G. P., and Smiraglia, C.: Surface energy budget and melt amount for the years 2009 and 2010
356 at the Forni Glacier (Italian Alps, Lombardy). *Geogr. Fis. Din. Quat.*, 35, 69–77, 2012b.
- 357 Senese, A., Maugeri, M., Vuillermoz, E., Smiraglia, C., and Diolaiuti, G.: Using daily air temperature thresholds to evaluate
358 snow melting occurrence and amount on Alpine glaciers by T-index models: the case study of the Forni Glacier (Italy).
359 *The Cryosphere*, 8, 1921–1933, 2014. www.the-cryosphere.net/8/1921/2014/
- 360 Senese, A., Maugeri, M., Ferrari, S., Confortola, G., Soncini, A., Bocchiola, D., and Diolaiuti, G.: Modelling shortwave and
361 longwave downward radiation and air temperature driving ablation at the Forni Glacier (Stelvio National Park, Italy).
362 *Geogr. Fis. Dinam. Quat.*, 39 (1), 89–100, 2016. DOI 10.4461/GFDQ. 2016.39.9
- 363 Super, A.B. and Holroyd III, E.W.: Snow accumulation algorithm for the WSR-88D radar: Second annual report. Bureau
364 Reclamation Tech. Rep. R-97-05, U.S. Dept. of Interior, Denver, CO, 77 pp., 1997. [Available from National Technical
365 Information Service, 5285 Port Royal Rd., Springfield, VA 22161.]
- 366 Smiraglia, C. and Diolaiuti, G.: Epiglacial morphology. In Singh VP, Haritashya UK, Singh P eds *Encyclopedia of Snow, Ice*
367 *and Glaciers* Springer, Berlin, 2011.
- 368 Urbini, S., Zirizzotti, A., Baskaradas, J., Tabacco, I.E., Cafarella, L., Senese, A., Smiraglia, C., and Diolaiuti, G.: Airborne
369 Radio Echo Sounding (RES) measures on Alpine Glaciers to evaluate ice thickness and bedrock geometry: preliminary
370 results from pilot tests performed in the Ortles Cevedale Group (Italian Alps). *Annals of Geophysics*, 60(2), 0226, 2017.



- 371 Wetzol, S.W. and Martin, J.E.: An operational ingredients-based methodology for forecasting midlatitude winter season
372 precipitation. *Wea. Forecasting*, 16, 156–167, 2001.
- 373 Work, R.A., Stockwell, H.J., Freeman, T.G., and Beaumont, R.T.: Accuracy of field snow surveys, Tech. Rep. 163, U.S.
374 Army Cold Reg. Res. and Eng. Lab., Hanover, N. H., 1965.
- 375 WMO Solid Precipitation Measurement Intercomparison: Final report. WMO/TD - No. 872. Instruments and observing
376 methods, Report No. 67, 202 pp, 1998.
- 377 WMO: Guide to Meteorological Instruments and Methods of Observation – WMO-No. 8 - Seventh edition, 2008.
378



379 Table 1: Instrumentation at the Forni Glacier with instrument name, measured parameter, manufacturer, and starting date.

Instrument name	Parameter	Manufacturer	Date
Babuc ABC	Data logger	LSI LASTEM	Sept. 2005
CR200	Data logger	Campbell	May 2014
CR1000	Data logger	Campbell	May 2014
Sonic ranger SR50	Snow depth	Campbell	Sept. 2005
Sonic ranger USH8	Snow depth	Sommer	May 2014
Snow pillow	SWE	Park Mechanical Inc.	May 2014
Thermo-hygrometer	Air temperature and humidity	LSI LASTEM	Sept. 2005
Barometer	Atmospheric pressure	LSI LASTEM	Sept. 2005
Net Radiometer CNR1	Short and long wave radiation fluxes	Kipp & Zonen	Sept. 2005
Pluviometer unheated	Liquid precipitation	LSI LASTEM	Sept. 2005
Anemometer 05103V	Wind speed and direction	Young	Sept. 2005

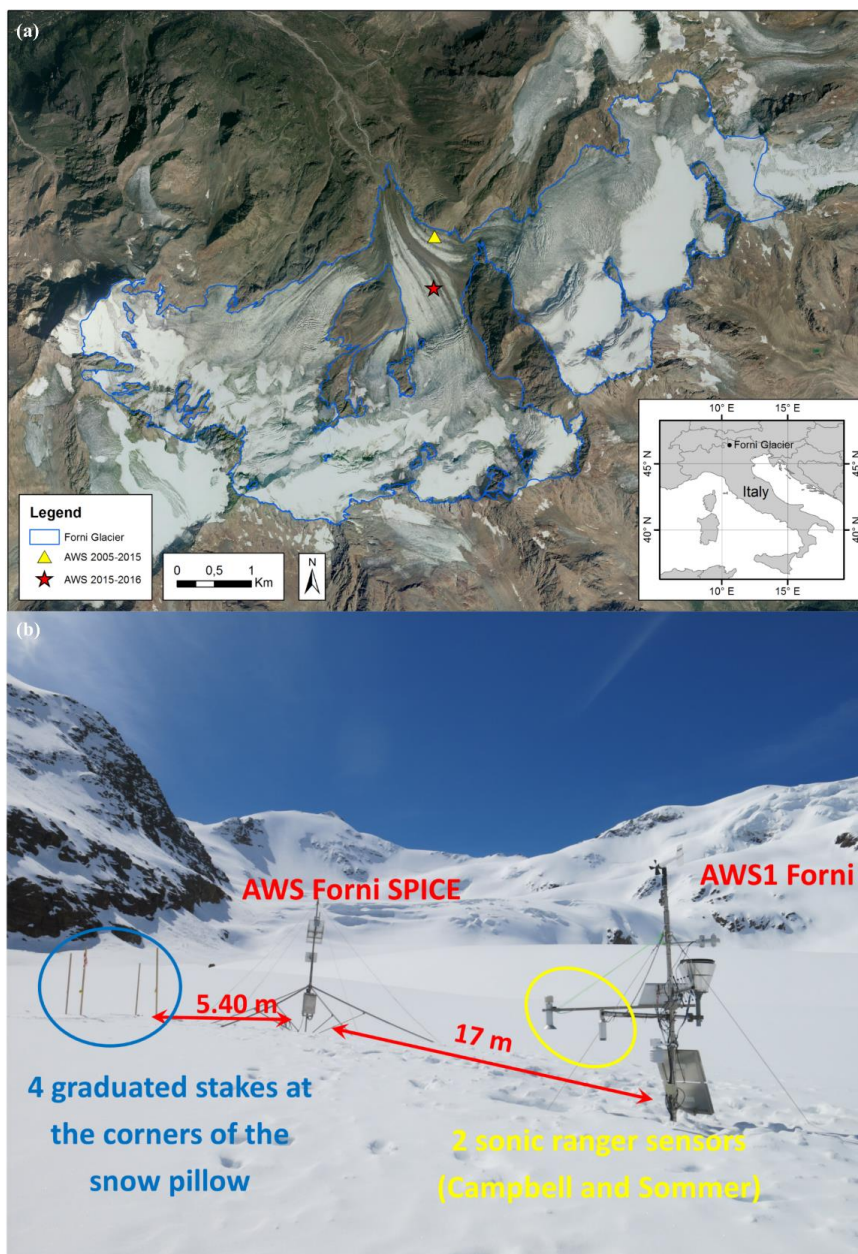
380



381 Table 2: For each snow pit measurement, *SWE* values (in m w.e.) are reported. The values are obtained by applying fresh
 382 snow density ranging from 100 to 180 kg m⁻³. In the last column is reported the value measured by snow pits.

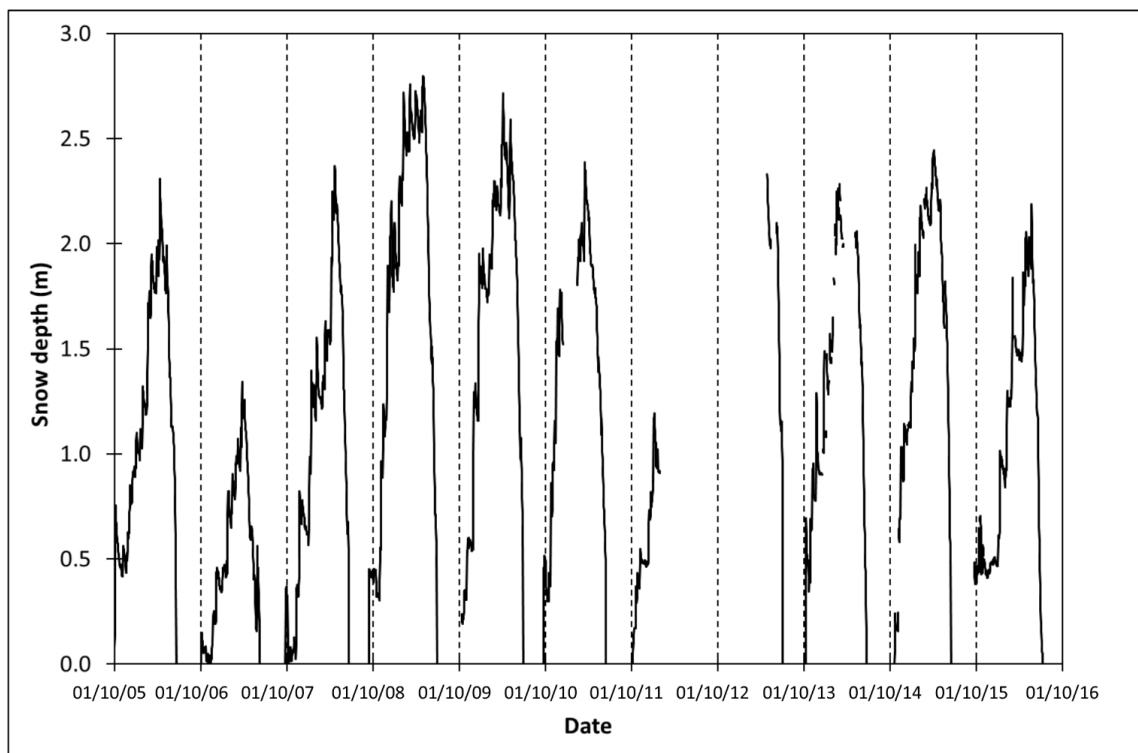
	100	120	140	160	180	Snow pit
24/01/06	0.229	0.275	0.321	0.367	0.413	0.337
02/03/06	0.335	0.402	0.469	0.536	0.603	0.430
30/03/06	0.421	0.505	0.589	0.673	0.757	0.619
07/05/08	0.492	0.590	0.688	0.787	0.885	0.690
21/02/09	0.427	0.513	0.598	0.684	0.769	0.650
27/03/10	0.410	0.492	0.573	0.655	0.737	0.640
25/04/11	0.530	0.636	0.742	0.848	0.953	0.770
01/05/12	0.437	0.525	0.612	0.700	0.787	0.615
25/04/13	-	-	-	-	-	0.778
06/05/14	0.337	0.404	0.472	0.539	0.607	1.043
20/02/15	0.363	0.436	0.508	0.581	0.653	0.555

383



384
385
386
387
388
389
390

Figure 1: (a) The study site. The yellow triangle indicates the location of the AWS1 Forni and the Forni AWS SPICE until November 2015. The red star refers to the actual location after securing the stations. (b) AWS1 Forni (on the right) and AWS Forni SPICE (on the left) photographed from the North-East on 6th May 2014 (immediately after the installation of the AWS Forni SPICE). The distances between the stations are shown.

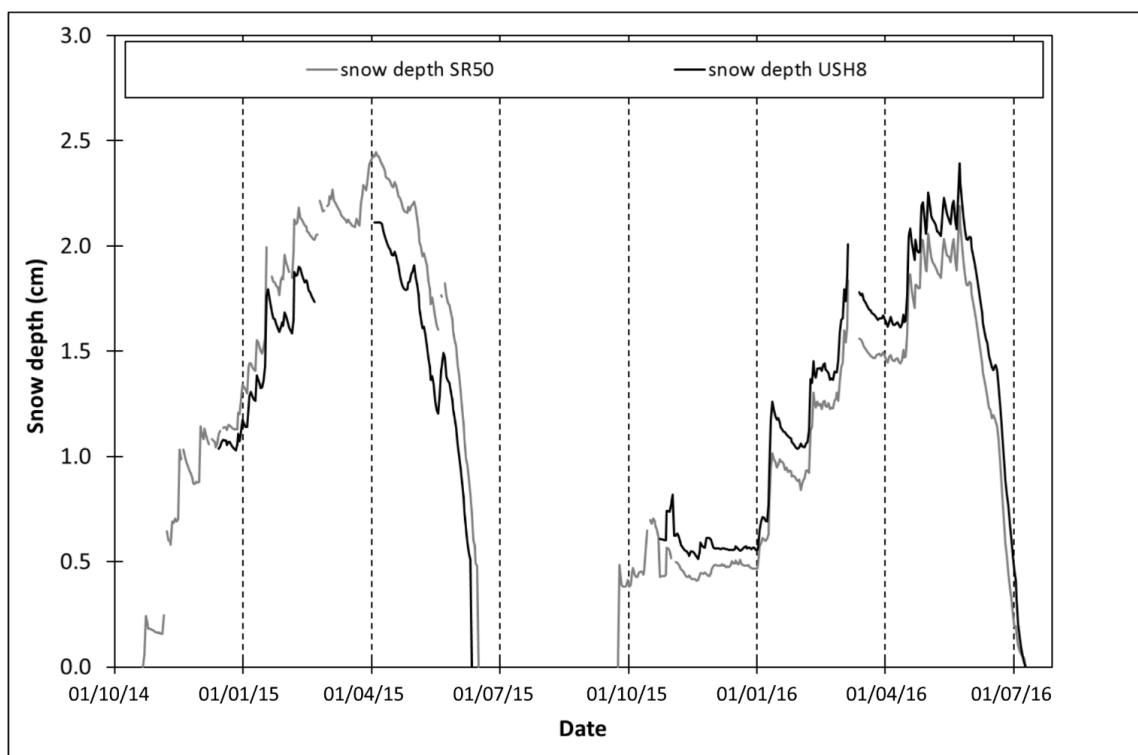


391

392 **Figure 2: Snow depth measured by the Campbell SR-50 sonic ranger at the AWS1 Forni from 1st October 2005 to 30th**

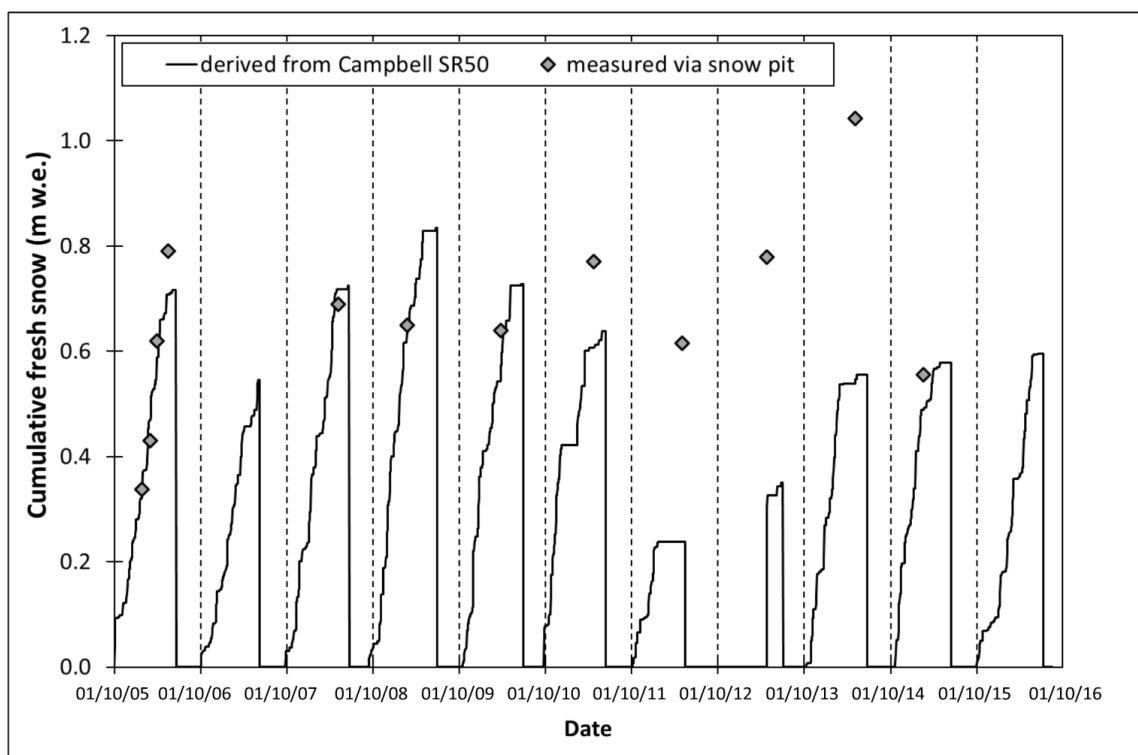
393 **Septher 2016. The dates shown are dd/mm/yy.**

394



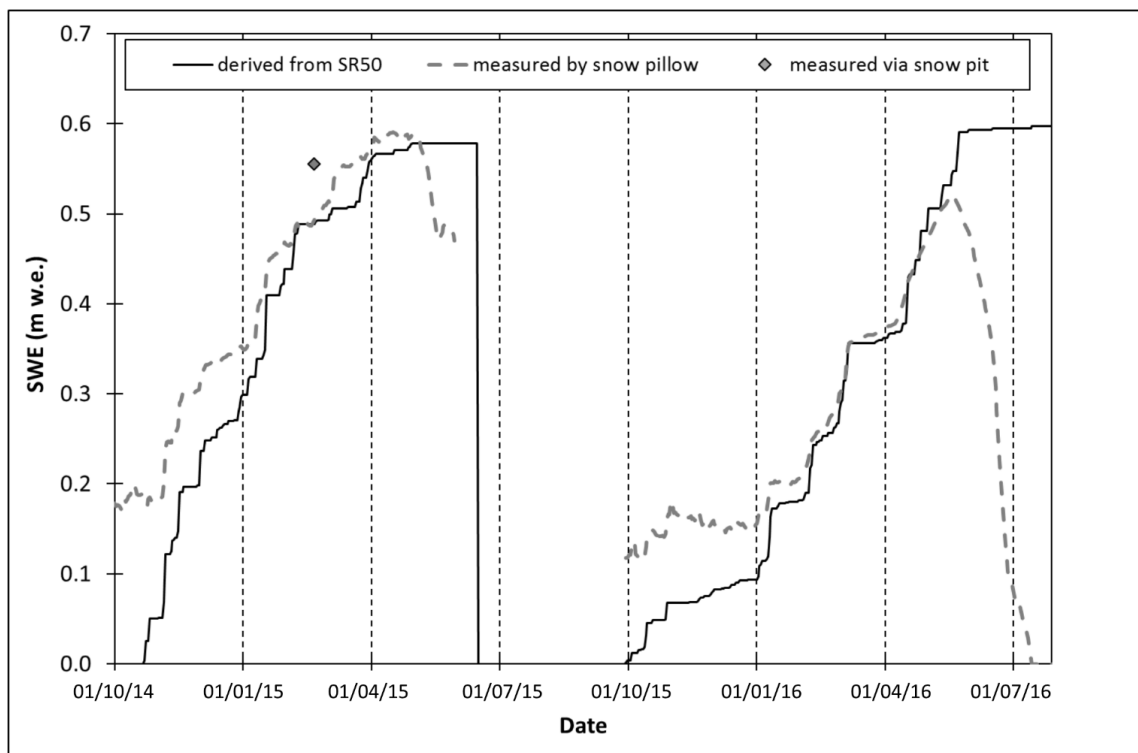
395
396
397
398

Figure 3: Snow depth data measured by Campbell SR50 and Sommer USH8, from October 2014 to July 2016. The dates shown are dd/mm/yy.



399
400
401
402

Figure 4: SWE data derived from snow depth by the Campbell SR50 and measured by snow pits from 1st October 2005 to 30th September 2016. The dates shown are dd/mm/yy.

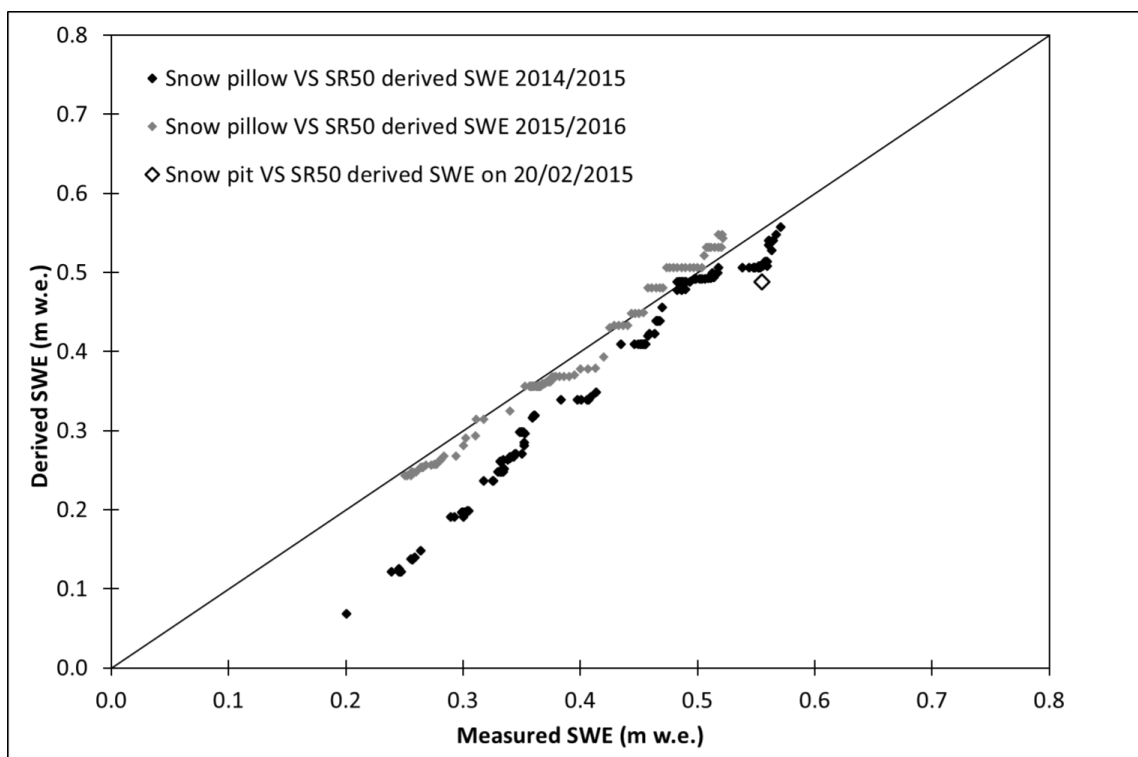


403

404 **Figure 5: SWE data derived from snow depth measured by Campbell SR50 and measured by snow pits and snow**
405 **pillow from October 2014 to July 2016. The dates shown are dd/mm/yy.**

406

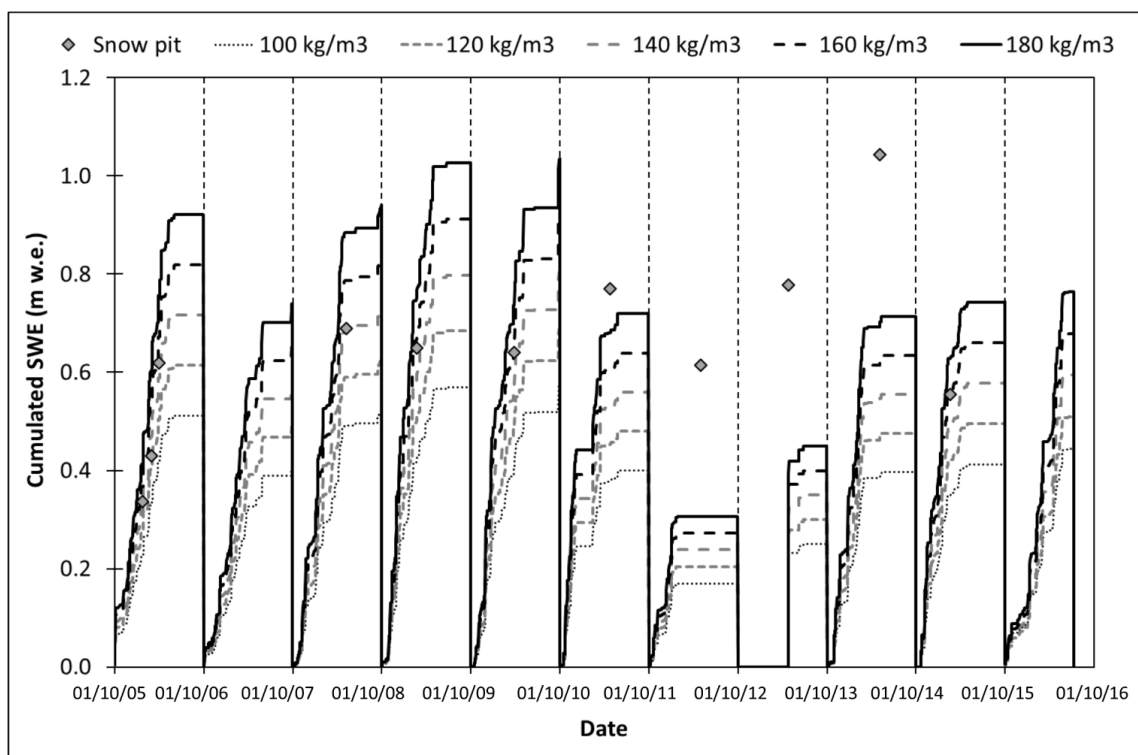
407



408

409 **Figure 6: Scatter plots showing SWE measured by snow pillow and snow pit and derived applying Eq. (2) to data**
410 **acquired by Campbell SR50. Two accumulation periods of measurements are shown from November 2014 to March**
411 **2015 and from February 2016 to May 2016. Every dot represents a daily value.**

412



413

414 **Figure 7: Comparison among SWE values derived from snow depth data acquired by SR50 sonic ranger (applying**
415 **different values of fresh snow density) and SWE values measured by snow pits from 2005 to 2016. The dates shown**
416 **are dd/mm/yy.**